

Enhancing the Accuracy of Ab Initio Molecular Dynamics by Fine Tuning of Effective Two-Body Interactions: Acetonitrile as a Test Case

Nuno Barbosa, Marco Pagliai, Sourab Sinha, Vincenzo Barone, Dario Alfè, and Giuseppe Brancato*



Cite This: *J. Phys. Chem. A* 2021, 125, 10475–10484



Read Online

ACCESS |



Metrics & More

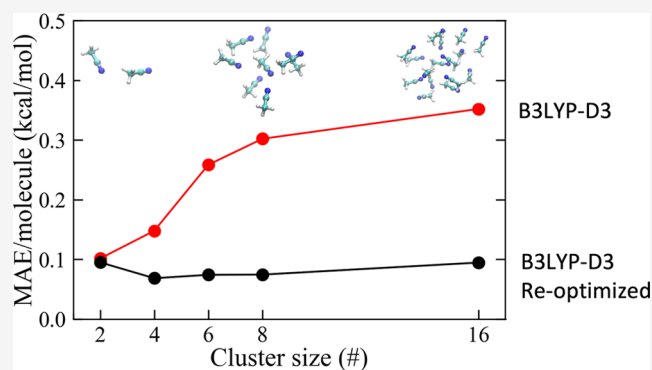


Article Recommendations



Supporting Information

ABSTRACT: Grimme's dispersion-corrected density functional theory (DFT-D) methods have emerged among the most practical approaches to perform accurate quantum mechanical calculations on molecular systems ranging from small clusters to microscopic and mesoscopic samples, i.e., including hundreds or thousands of molecules. Moreover, DFT-D functionals can be easily integrated into popular *ab initio* molecular dynamics (MD) software packages to carry out first-principles condensed-phase simulations at an affordable computational cost. Here, starting from the well-established D3 version of the dispersion-correction term, we present a simple protocol to improve the accurate description of the intermolecular interactions of molecular clusters of growing size, considering acetonitrile as a test case. Optimization of the interaction energy was performed with reference to diffusion quantum Monte Carlo calculations, successfully reaching the same inherent accuracy of the latter (statistical error of ~ 0.1 kcal/mol per molecule). The refined DFT-D3 model was then used to perform *ab initio* MD simulations of liquid acetonitrile, again showing significant improvements toward available experimental data with respect to the default correction.



1. INTRODUCTION

Poor description of van der Waals interactions by standard density functional theory (DFT) approximations has boosted the development of new improved theoretical and empirical models,^{1–4} especially for the treatment of extended molecular systems of great interest for life and materials sciences (see ref 5 for a review). Among others, the so-called dispersion-corrected DFT (DFT-D) methods, as proposed by Grimme and co-workers,^{4,6,7} have emerged as some of the most versatile, accurate, and computationally efficient approaches for modeling and simulating large molecular systems. The DFT-D3⁴ approach, in particular, is a well-established atom pairwise correction, which has been successfully tested for calculations on various molecular complexes and architectures.^{8,9} The general assumption underlying all of the DFT-D variants is that the dispersion energy can be added to the electronic energy obtained from the standard Kohn–Sham DFT as a “classical” (i.e., independent from the electronic structure) interatomic potential, including two or more high-order multipole interaction terms (typically, C_6/R ,⁶ C_8/R ,⁸ and so on) modulated by further damping functions and scaling factors. Such semiclassical corrections have proved very valuable, if not unavoidable with respect to the uncorrected DFT, for the proper calculations of structural as well as thermodynamic properties of a wide range of chemical systems.^{6,8,9} In fact, it

has been unequivocally shown that well-known and widely used DFT approximations (e.g., B3LYP^{10,11}) can fail badly when used to model simple molecular complexes dominated by van der Waals interactions.⁵ However, DFT-D models can deliver satisfactory results only if carefully parametrized by fitting a few adjustable parameters, which are generally dependent on the specific density functional (parameters for more than 80 functionals are available), to accurate reference data. In this context, typical benchmark sets range from high-level coupled cluster calculations of small organic complexes¹² to experimentally determined association energies of large supramolecular systems¹³ and to sublimation energies of molecular crystals,¹⁴ though experimental energies always require some a posteriori corrections to be compared to single-point energy calculations. At least for medium-sized molecular systems (i.e., few hundred atoms), (local) correlated wave function and quantum Monte Carlo methods are nowadays feasible,^{15,16} with the latter showing a favorable

Received: August 26, 2021

Revised: November 16, 2021

Published: November 29, 2021



cubic scaling with the number of electrons. A common feature of molecular test sets is the use of isolated equilibrium structures to avoid the perturbing effects of thermal fluctuations and chemical environment. This is a sensible choice for systematically assessing a large number of different electronic structure models toward a balanced selection of assorted chemical systems. However, in our opinion, alternative approaches could be more convenient for developing dispersion-corrected DFT models tailored to the accurate description of condensed-phase systems, especially liquids. This is an active area of interest since DFT-based *ab initio* molecular dynamics (AIMD) techniques offer the advantage of an explicit electronic treatment as compared to force-field-based simulations, though limited in their time-scale reach. In past studies, for example, dispersion corrections have been successfully tested in AIMD simulations of liquid water,^{17,18} demonstrating the beneficial inclusion of London interactions for reproducing basic liquid properties.

Here, we aimed at assessing the use of DFT-D3 as an accurate computational model for the consistent description of noncovalent interactions of a given molecular system when going from microscopic clusters to the liquid phase, taking acetonitrile as a test case. We adopted the D3 version since it is more popular among QM and AIMD software packages but the same computational protocol could be easily extended to other updated DFT-D variants, such as DFT-D4.^{19,20} To this end, we devised a computational protocol summarized in Figure 1. In contrast to typical test sets that include mostly equilibrium structures and binary systems, we generated multiple nonequilibrium configurations of molecular clusters of growing size, ranging from dimers to hexadecamers, as obtained from the corresponding classical molecular dynamics (MD) simulation of liquid acetonitrile. For this task, we think that carefully developed force fields are particularly well suited for sampling liquid-like uncorrelated configurations. Overall, the interaction energies of 500 cluster configurations were tested toward diffusion quantum Monte Carlo (DMC) benchmark data purposely performed for this work. In fact, we believe that validating DFT-D approaches on molecular aggregates of variable dimension may help to emphasize possible flaws in the description of the London dispersion interactions. Then, we refined the D3 parametrization of two very popular DFT approximations, i.e., BLYP and B3LYP, aiming at improving the agreement with DMC interaction energies. We found that optimization of the dispersion-correction term (namely, the S_8 parameter) accounting for the $n > 6$ order multipole interactions at short/medium-range distances led to a significant improvement of the results, which showed mean absolute deviations within the accuracy of reference data (0.1 kcal/mol per molecule). Finally, the optimized BLYP-D3 model, as well as the default one and the standard uncorrected BLYP, were used to perform *ab initio* MD simulations of liquid acetonitrile, again showing remarkable improvements toward available experimental data.

2. METHODS

2.1. Molecular Cluster Configurations. Various molecular cluster configurations were obtained by extracting molecular assemblies of different sizes (i.e., from dimers to hexadecamers) from a large number of snapshots issued from an NpT ensemble MD simulation of liquid acetonitrile carried out at normal conditions ($T = 300$ K, $p = 1$ atm). The recently optimized acetonitrile molecular model of Nikitin and

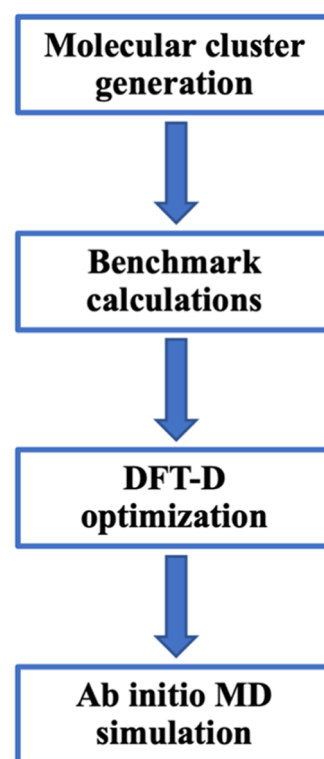


Figure 1. Basic steps of the computational protocol proposed in this study. Molecular cluster generation: representative nonequilibrium configurations of molecular clusters of growing size are generated from MD simulations of condensed-phase systems based on reliable force fields; benchmark calculations: reference interaction energies of small to large clusters are obtained from high-level quantum mechanical calculations (e.g., diffusion Monte Carlo); DFT-D optimization: DFT dispersion-correction terms are optimized against benchmark data; *ab initio* MD simulation: condensed-phase system simulations are carried out at the DFT-D level.

Lyubartsev²¹ was adopted for this purpose, since it can fairly well reproduce all main properties of the liquid, such as structure, density, and thermodynamics. All bonds were constrained using the LINCS²² algorithm and simulations were performed using a time step of 1 fs. As a result, the following cluster configurations were obtained: 150 dimers (i.e., 2mer), 150 tetramers (i.e., 4mer), 100 hexamers (i.e., 6mer), 50 octamers (i.e., 8mer), and 50 hexadecamers (i.e., 16mer). The GROMACS²³ software package was used for all MD simulations.

2.2. Diffusion Monte Carlo. Diffusion Monte Carlo calculations were performed with the Casino code²⁴ using trial wavefunctions of the Slater–Jastrow type

$$\Psi_T(\mathbf{R}) = D^\uparrow D^\downarrow e^J \quad (1)$$

where D^\uparrow and D^\downarrow are Slater determinants of up- and down-spin single-electron orbitals and e^J is the so-called Jastrow factor, which is the exponential of a sum of one-body (electron–nucleus), two-body (electron–electron), and three-body (electron–electron–nucleus) terms.²⁵ Imaginary time evolution of the Schrödinger equation was performed with the usual short time approximation using the T-move scheme.²⁶

We used Dirac–Fock pseudopotentials (PP) for C, N, and H.²⁷ The C and N PPs have a frozen He core and core radii of 0.58 and 0.44 Å, respectively. The H PP has a core radius of 0.26 Å. The single particle orbitals were obtained by DFT

plane-wave (PW) calculations using the local density approximation (LDA) and a PW cutoff of 500 Ry, using the pwscf package,²⁸ and reexpanded in terms of B-splines,²⁹ using the natural B-spline grid spacing given by $a = \pi/G_{\max}$, where G_{\max} is the length of the largest vector employed in the PW calculations. The PW calculations were performed by putting the systems in boxes with at least 5 Å of empty space in each direction. The DMC calculations were then performed without periodic boundary conditions (PBC), using the Ewald interaction to model electron–electron interactions. Note that switching off PBC eliminates finite size effects due to periodic images, which in a many-body technique such as DMC would decay more slowly with the size of the simulation cell. To investigate convergence of the binding energy with respect to time step, we repeated the calculations on 10 different dimer configurations using time steps of 0.005 and 0.002 au, which showed differences in the binding energies of less than the statistical error of ~ 5 meV/dimer. We therefore decided to use a time step of 0.005 au.

2.3. DFT and Dispersion Corrections. In the next step of this study, single-point energy calculations at the DFT level of theory were carried out on the acetonitrile molecular clusters issued from MD simulations. DFT calculations were performed with Gaussian09³⁰ using a combination of Becke's exchange functional³¹ with the correlation function LYP^{32,33} and the B3LYP³⁴ hybrid functional. For the sake of comparison, also the M062X and the double-hybrid B2PLYP functionals were considered in a few calculations. 6-31+G(d,p), 6-31+D(2d,2p), and Dunning's correlation (aug-cc-pVTZ)³⁵ basis sets were used. Single-point energies were corrected using the original Grimme's D3 dispersion-correction term. Grimme and co-workers showed that D3 is less empirical than previous D1 and D2 corrections, showing a better overall accuracy, as well as dispersion coefficients computed explicitly.⁴ The total energy (i.e., including dispersion corrections) can be described as

$$E_{\text{DFT-D3}} = E_{\text{DFT}} - E_{\text{dis}} \quad (2)$$

where E_{dis} is expressed as neglecting the three-body or higher terms

$$E_{\text{dis}} = \sum_{a,b}^N \sum_{n=6,8,\dots} S_n \frac{C_n^{ab}}{r_{ab}^n} f_{d,n}(r_{ab}) \quad (3)$$

where C_n^{ab} is the n th-order dispersion coefficient (orders $n = 6, 8, \dots$) defined for any given atom pair (a, b) in the system, r_{ab} is the internuclear atom pair distance, $f_{d,n}(r_{ab})$ is a damping function introduced to avoid singularities at small interatomic distances, and S_n is the scaling factor (typically dependent on the DFT method). The damping function has the form

$$f_{d,n}(r_{ab}) = \frac{1}{1 + 6 \left(\frac{r_{ab}}{(S_{R,n} R_0^{ab})} \right)^{-\alpha_n}} \quad (4)$$

where $S_{R,n}$ is the order-dependent scaling factor of the cutoff radius R_0^{ab} and α_n is the steepness parameter. For a detailed discussion of the meaning and definition of all parameters, see ref 4. Here, we note that in practical implementations of DFT-D3, the n th order is usually truncated after $n = 8$ and most of the parameters are computed *ab initio* (C_6^{ab}), derived recursively (C_8^{ab}) or kept fixed (e.g., $S_{R,8}$ and S_6 are set to 1 for all DFT methods, except those accounting for dispersion energy). On the other hand, S_8 and $S_{R,6}$ are empirical parameters, which are adjusted based on the density functional

(e.g., $S_8 = 1.703$ and $S_{R,6} = 1.261$ for B3LYP; $S_8 = 1.682$ and $S_{R,6} = 1.094$ for BLYP). In particular, the S_8 scaling factor is considered to account implicitly for higher multipolar terms beyond the dipole–dipole contribution. For the purpose of further testing, the D3BJ³⁶ (which includes the Becke and Johnson damping function) and D4^{19,20} variants were also considered. In the latter case, the DFT-D4 standalone code available on GitHub was used for calculations.

2.4. Optimization Procedure. The optimization procedure of the dispersion-correction term (eq 3) was tailored to minimize the deviation in the computed cluster interaction energies between DMC and DFT as issued from calculations on large sets of molecular clusters of growing size ($n = 2-16$). For each cluster configuration, such an interaction energy deviation is defined by subtracting the one-body energy deviation, $\Delta E_{1\text{-body}}^n$, from the total interaction energy difference, ΔE^n , as follows

$$\Delta E^n - \Delta E_{1\text{-body}}^n \quad (5)$$

where

$$\begin{aligned} \Delta E^n &= (\Delta E_{\text{DFT}}^n - \Delta E_{\text{DMC}}^n) \\ \Delta E_{1\text{-body}}^n &= (\Delta E_{1\text{-body,DFT}}^n - \Delta E_{1\text{-body,DMC}}^n) \end{aligned} \quad (6)$$

while for the one-body and total interaction energy of the corresponding electronic structure calculation, we have

$$\begin{aligned} \Delta E_X^n &= E_X^n - nE_X^{\text{ref}} \\ \Delta E_{1\text{-body},X}^n &= \sum_i^n (E_X^i - E_X^{\text{ref}}) \end{aligned} \quad (7)$$

E_X^n is the total energy of the n th cluster (with $n = 2-16$) configuration computed at the X ($=$ DMC, DFT, DFT-D3) level of theory, E_X^{ref} is the energy of the isolated molecule at the reference geometry (according to the force-field model, geometry is as follows: CN = 1.157 Å, CC = 1.458 Å, CH = 1.090 Å, HCH = 109.5°, and HCC = 110.0°) computed at the same level of theory, and E_X^i is the energy of the isolated i th (with $i = 1 - n$) molecule (possibly distorted) taken from the cluster configuration. Note that in the present work, since the individual molecules of the generated cluster structures had nearly ideal (reference) geometry (i.e., all bonds were constrained), the contribution of the $\Delta E_{1\text{-body}}^n$ was found to be negligible (see below) and, therefore, it was ignored during the optimization procedure. Note that for the assessment of the S_8 scaling factor, a convenient optimization procedure could exploit a global fitting toward the results issued from all cluster systems. In the present case, however, the S_8 optimization performed through a simple grid search on the 8mer system led to a consistent correction readily extended to all other cluster sizes (vide infra).

2.5. Ab Initio Molecular Dynamics Simulations. *Ab initio* molecular dynamics (AIMD) simulations with the Born–Oppenheimer method were carried out with the QuickStep³⁷ module of the CP2K suite of programs³⁸ to study the structural and thermodynamic properties of liquid acetonitrile. The interaction potential was computed within density functional theory (DFT), employing the BLYP^{31,32} exchange and correlation functional. The TZV2P basis set in conjunction with Goedecker–Teter–Hutter (GTH)³⁹ pseudopotentials and a plane-wave cutoff of 400 Ry was adopted to describe the electronic structure of the systems. The BLYP-D3 method

proposed by Grimme et al.^{4,36} was employed to better describe the dispersion forces using both the default and the modified form of D3 (with the S_8 parameter multiplied by a 0.7253 factor, corresponding to 1.22). A further AIMD simulation was carried out without van der Waals corrections using standard BLYP. All simulations were performed using a fixed periodic cubic box with a 17.6982 Å edge containing 64 acetonitrile molecules, thus corresponding to the experimental density of 0.786 g/cm³. All systems were thermalized by rescaling the velocities at ambient temperature ($T = 300$ K), while performing constant-volume simulations with a time step of 0.1 fs for 8 ps.

3. RESULTS AND DISCUSSION

3.1. Assessment of the D3 Dispersion Energy Correction. In the present study, a large set of acetonitrile molecular clusters (i.e., 500 configurations) was considered to assess and then refine the effect of Grimme's D3 correction on the interaction energy computed at DFT (i.e., B3LYP and BLYP) level of theory, as compared to high-level DMC calculations. To assess the extent of the correction, we report in Figure 2a the discrepancy between standard and corrected

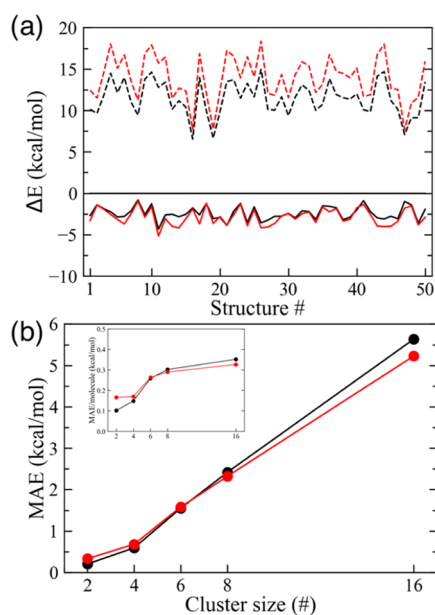


Figure 2. (a) B3LYP (black) and BLYP (red) interaction energy deviations with respect to DMC as computed with (solid line) and without (dashed line) default Grimme's D3 correction on a set of 50 representative configurations of the acetonitrile 8mer cluster. (b) Mean absolute error (MAE) of B3LYP-D3 (black) and BLYP-D3 (red) energy deviations with respect to DMC on acetonitrile clusters of growing size (i.e., from 2mer to 16mer); inset: MAE per molecule.

B3LYP and BLYP calculations with respect to DMC on a number of representative 8mer structures using the 6-31+G(d,p) basis set in both cases. While standard B3LYP and BLYP underestimate, on average, the total interaction energy by about 11.5 and 14.4 kcal/mol, the corresponding DFT-D3 calculations appear to overestimate the same energy by 2.4 kcal/mol, thus showing a notable improvement with respect to the uncorrected DFT energies. This result, as expected, demonstrates the capability of DFT-D3 to effectively recover the missing dispersion energy. Also, it is worth noting the decrease on the energy fluctuations upon introduction of

the dispersion corrections, the standard deviation being reduced by half (from ~ 2 kcal/mol to less than ~ 1 kcal/mol). Interestingly, when DFT-D3 calculations were performed by setting the $n = 8$ order term to zero (i.e., $S_8 = 0$) in eq 3, the overall energy correction was reduced by half (i.e., on average 48%, Figure S1), a result showing that, at least for acetonitrile, the latter contribution is quantitatively similar to the $n = 6$ term. For the sake of comparison, we carried out further calculations at M062X-D3 and B2PLYP-D3 levels, which again showed some deviations with respect to benchmark calculations, though less pronounced for the former functional (Figure S2). Moreover, we also tested the D3BJ³⁶ variant, which includes the Becke and Johnson damping function, and the D4^{19,20} variant, which has updated C6 coefficients, BJ damping function, and a three-body interaction term. The results are reported in Figure S3. We noticed that the use of the BJ damping function, even though it is generally recommended, did not change the interaction energy of the acetonitrile clusters significantly with respect to the standard "zero damping" formula, in line with what was observed in ref 36 for noncovalent systems. D4 showed, on the other hand, a sensible improvement in the description of the dispersion interactions, though deviations with respect to reference data were still present (mean absolute error (MAE) = 1.16 kcal/mol for B3LYP and MAE = 0.63 kcal/mol for BLYP). In this case, it is interesting to observe that the three-body term appeared to have a negligible effect on D4 results (Figure S3a).

The previous results refer to total interaction energies (ΔE^8), including the one-body term ($\Delta E_{1\text{-body}}^8$), were reported. As a matter of fact, this was justified by the observation that energy deviations of individual monomers from test calculations were very small (i.e., average error was 0.05 kcal/mol, Figure S4), possibly canceling each other in larger clusters. The role of $\Delta E_{1\text{-body}}^8$ in the context of this work was reconsidered in the following.

To further assess the impact of the default D3 correction on clusters of variable size and to better estimate the effect of the basis set, we carried out similar calculations at B3LYP-D3 and BLYP-D3 level of theory by considering molecular structures ranging from dimers to hexadecamers and by comparing the 6-31+G(d,p), 6-31+D(2d,2p), and aug-cc-pVTZ basis sets. The results are summarized in Table S1 and Figure 3. First of all, the steady increase of the energy deviation between DFT-D3 and DMC with the system size is apparent: the mean absolute error (MAE) shows a roughly linear trend going from 2mer to 16mer, with a parallel increase of both B3LYP and BLYP results as depicted in Figure 2b. For the largest clusters considered (i.e., 16mer), MAE is over 5 kcal/mol. More specifically, the MAE per molecule does show an increase from 0.1 to 0.2 kcal/mol (i.e., 2mer) to over 0.3 kcal/mol (16mer) (see inset of Figure 2b). Although such energy discrepancies seem not too large, the observed increase with the cluster size suggests that the overestimation of the dispersion interaction by DFT-D3 may become more relevant when going to larger acetonitrile clusters or to mesoscopic samples. Overall, the same trend was observed by comparing the three basis sets, with minor changes in the energy deviations between DFT-D3 and DMC (note, however, that the most extended 16mer cluster was excluded in the comparison). Therefore, although present, the basis-set superposition error (BSSE) in this case appeared to be of less importance with respect to the inaccuracy of the combined density functional/dispersion-

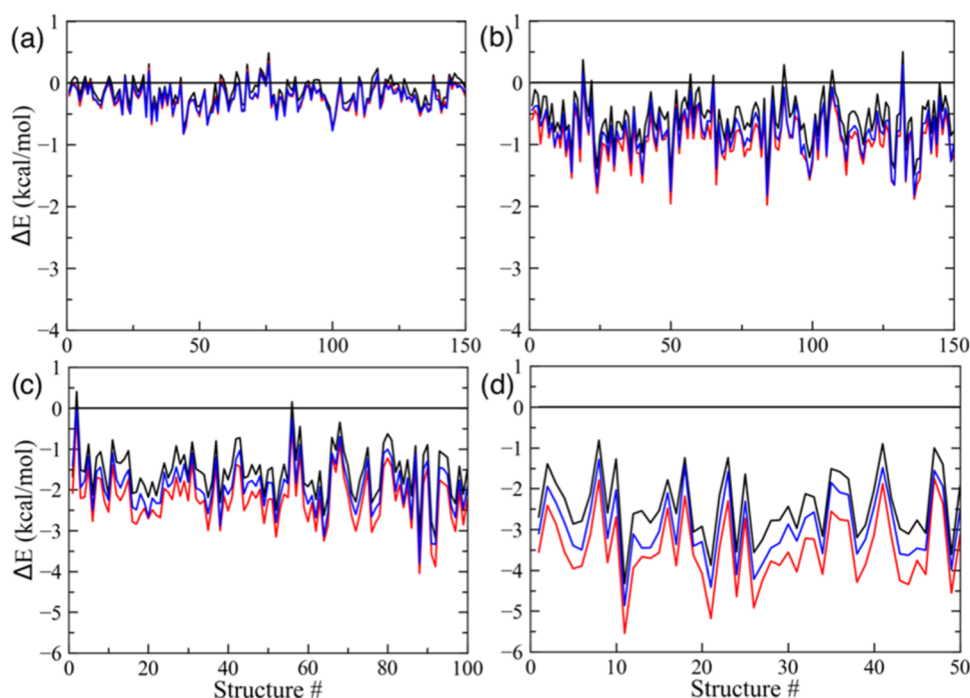


Figure 3. B3LYP-D3 interaction energy deviations with respect to DMC as computed with the 6-31+G(d,p) (black), 6-31+D(2d,2p) (red), and aug-cc-pVTZ (blue) basis sets on a set of acetonitrile cluster configurations: (a) 2mer, (b) 4mer, (c) 6mer, and (d) 8mer.

correction model. Incidentally, the smallest basis set reported the lowest MAE, possibly due to some fortuitous but systematic error compensation. In the following optimization procedure, for the sake of convenience, we therefore decided to employ the 6-31+G(d,p) basis set. In view of the observed minor differences with respect to the basis-set choice (i.e., for B3LYP, MAE per molecule is 0.06 kcal/mol between 6-31+G(d,p) and aug-cc-pVTZ), the optimization procedure is considered to be essentially not dependent on the basis set. On the other hand, when an even smaller basis set was considered for the 8mer in test calculations (i.e., 6-31G*), non-negligible deviations with respect to the reference basis set (i.e., aug-cc-pVTZ) appeared (Figure S5).

3.2. Optimization of the D3 Term. At this point, one can ask if the discrepancy between DFT-D3 and DMC can be significantly reduced by refining one or more parameters of the D3 empirical dispersion term (eq 3) and whether such an optimization can improve the results consistently for molecular samples of variable size or be beneficial only for a given cluster dimension. Since the $n = 8$ order term accounts for a good extent of the overall dispersion energy correction (Figure S1) and the S_8 scaling factor is one of the few empirically adjustable parameters of the Grimme's D3 version (eq 3), we decided to refine this parameter by focusing specifically on two popular hybrid and gradient-corrected density functionals, B3LYP and BLYP, respectively, in combination with the 6-31+G(d,p) basis set. Optimization was performed with the purpose of achieving a better agreement between DFT and DMC benchmark calculations. The default values of S_8 for BLYP-D3 and B3LYP-D3 are 1.682 and 1.703, respectively. In preliminary tests, we focused only on the octamer cluster since it represents a good compromise between the molecular size and computational cost (i.e., especially for DMC calculations). In particular, S_8 was refined to minimize the MAE issued from calculations on this cluster. The results of MAE obtained from B3LYP-D3 calculations are reported in Table S2, whereas absolute energy

deviations for selected S_8 values are depicted in Figure 4. Data presented in Figure 4 are obtained with the same functional

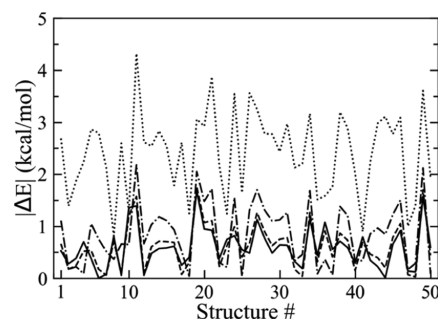


Figure 4. B3LYP-D3 (absolute) interaction energy deviations with respect to DMC as computed by setting the S_8 scaling factor to 1.703 (default, dotted), 1.35 (dot-dashed), 1.25 (dashed), and 1.22 (solid) on a set of 50 representative configurations of the acetonitrile 8mer cluster.

and basis set (i.e., B3LYP-D3/6-31+G(d,p)), differing only for the S_8 parameter. The first set of data were generated with the default value ($S_8 = 1.703$) and show poor agreement with benchmark values as seen above (MAE = 2.4 kcal/mol). Considering the trend reported in Figure S1, it was expected that refinement of S_8 should lead to a decrease in the default value ($S_8 < 1.7$) to reduce the observed overestimation of the interaction energy. By changing the S_8 parameter from the default value (i.e., 1.703) to ~ 1.20 , a significant decrease of the MAE of about four times, from 2.4 to 0.6 kcal/mol, was obtained for the 8mer cluster (Table S2). Although the results for $S_8 = 1.18$ – 1.23 appeared rather similar, we took $S_8 = 1.22$ as the optimal value of the scaling factor. In this case, the MAE per molecule is only 0.07 kcal/mol, a satisfactory result considering that the estimated accuracy of DMC is about 0.1 kcal/mol. In addition, the standard deviation was somewhat

reduced (from 0.80 to 0.69 kcal/mol), as displayed in Figure 4. Despite the very low MAE, we decided to better estimate the interaction energy of the five 8mer configurations leading to maximum energy deviations (i.e., $|\Delta E|$ greater than 1 kcal/mol) by subtracting the contribution of the one-body energy term ($\Delta E_{1\text{-body}}^n$). The results are reported in Figure 5, which

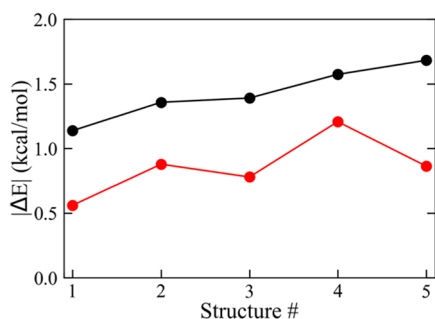


Figure 5. B3LYP-D3 (absolute) interaction energy deviations with respect to DMC as computed by setting the S_8 scaling factor to 1.22, including (black) or subtracting (red) the one-body energy term ($\Delta E_{1\text{-body}}^n$) as in eq 5, on five selected configurations of the acetonitrile 8mer cluster showing the largest energy deviations ($|\Delta E| > 1$ kcal/mol). Without the $\Delta E_{1\text{-body}}^n$ term, $|\Delta E|$ is reduced by about 40% on average.

shows a marked reduction of the energy deviation by about 40%, with $|\Delta E| < 1$ kcal/mol in all cases except one. Hence, while the contribution to the total energy deviation of the one-body term was generally small for the tested acetonitrile cluster configurations (about 0.05 kcal/mol per monomer) and could be safely ignored in the optimization procedure outlined above, an even better agreement with DMC benchmark calculations was achieved by properly taking into account $\Delta E_{1\text{-body}}^n$ in the

evaluation of the interaction energies. Nevertheless, since the results of the optimized DFT-D3 model appeared to be within the limit of accuracy of DMC (MAE/molecule = ~ 0.1 kcal/mol), the effect of $\Delta E_{1\text{-body}}^n$ was neglected in the following.

Furthermore, B3LYP-D3 calculations with the refined scaling factor ($S_8 = 1.22$) were carried out for all clusters considered in the present work to validate the improvement in the computed interaction energy on molecular assemblies of growing size. The obtained results were compared with default S_8 calculations and reported in Table 1, Figures 6 and 7. Overall, we noted a remarkable agreement with the DMC results at any size, energy deviations being effectively reduced by a factor of 4 in the largest clusters. Moreover, the MAE per molecule never exceeded 0.1 kcal/mol, thus showing a rather flat trend versus the system size as depicted in Figure 7. These findings suggest that the observed improvement could be reasonably projected onto even larger clusters and/or liquid phase systems for which high-level quantum mechanical calculations are unfeasible.

The same general approach was employed to obtain an effective S_8 parameter to be used in combination with the BLYP functional. Upon optimization, a value of 1.18 was set for the present scaling factor (Table S3). As shown in Table 1, it was found that MAE became as low as 0.69 kcal/mol for the octamer cluster after applying the new refined S_8 parameter, meaning a 70% improvement when compared to the default parameter (i.e., from 2.32 to 0.69 kcal/mol). By extending the refined BLYP-D3 model to all acetonitrile configurations, we again found an overall better agreement with respect to DMC (Table 1).

3.3. Liquid Acetonitrile: Structural Properties and Pressure. Structural properties of liquid acetonitrile were determined experimentally by means of X-ray and neutron diffraction studies.^{40,41} Previously, such results were adopted as

Table 1. Error (Err), Mean Square Error (MSE), Mean Absolute Error (MAE), and MAE per Molecule (MAE/molecule) of B3LYP-D3/6-31+G(d,p) and BLYP-D3/6-31+G(d,p) Interaction Energy Deviations with respect to DMC as Computed by Setting the S_8 Scaling Factor to 1.22 and Default (1.703) on all Acetonitrile Clusters (i.e., from 2mer to 16mer) Considered in this Study

		B3LYP-D3		BLYP-D3	
		default	$S_8 = 1.22$	default	$S_8 = 1.18$
2mer	Err	-0.1394	0.0362	-0.2143	-0.0523
	MSE	0.0649	0.0546	0.1293	0.0967
	MAE	0.2032	0.1900	0.2850	0.2533
	MAE/molecule	0.1016	0.0950	0.1425	0.1266
4mer	Err	-0.5698	0.0735	-0.6472	0.0213
	MSE	0.4592	0.1219	0.6500	0.2082
	MAE	0.5918	0.2738	0.6800	0.3583
	MAE/molecule	0.1479	0.0684	0.1700	0.0896
6mer	Err	-1.5405	-0.2307	-1.5588	-0.1976
	MSE	2.7460	0.3296	2.9953	0.4812
	MAE	1.5517	0.4448	1.5798	0.5305
	MAE/molecule	0.2586	0.0741	0.2633	0.0884
8mer	Err	-2.4171	-0.1734	-2.3207	0.0110
	MSE	6.4864	0.5092	6.2462	0.6806
	MAE	2.4171	0.5961	2.3207	0.6904
	MAE/molecule	0.3021	0.0745	0.2901	0.0863
16mer	Err	-5.634	1.2989	-5.2268	1.9787
	MSE	33.849	3.3564	29.7230	5.7886
	MAE	5.6342	1.5144	5.2268	2.0501
	MAE/molecule	0.3521	0.0946	0.3267	0.1281

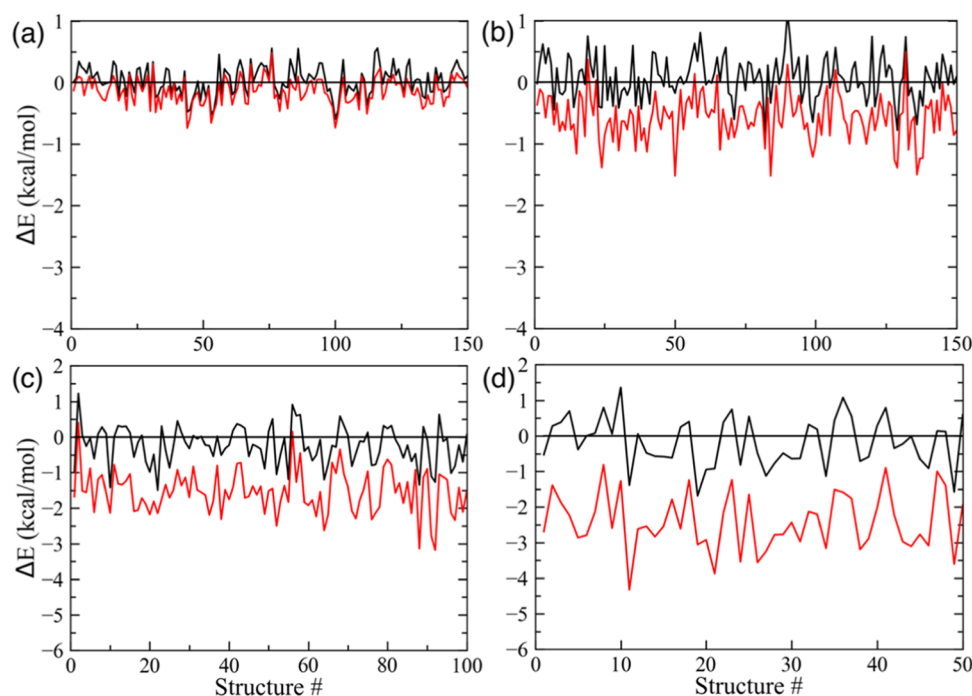


Figure 6. B3LYP-D3/6-31+G(d,p) interaction energy deviations with respect to DMC as computed by setting the S_8 scaling factor to 1.22 (black) and 1.703 (default, red) on a set of acetonitrile cluster configurations: (a) 2mer, (b) 4mer, (c) 6mer, and (d) 8mer.

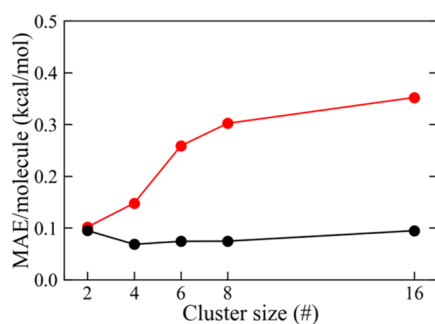


Figure 7. Mean absolute error (MAE) per molecule of B3LYP-D3/6-31+G(d,p) with respect to DMC as computed by setting the S_8 scaling factor to 1.22 (black) and 1.703 (default, red) on acetonitrile clusters of growing size (i.e., from 2mer to 16mer).

a benchmark for developing effective interaction potentials for molecular simulations.^{21,42–47} In particular, it was observed that the models proposed by Böhm et al.^{42,43} and Edwards et al.⁴⁴ provided structural information in very good agreement with the experiments. Some liquid acetonitrile properties, such as density, dielectric constant, and enthalpy of vaporization are accurately reproduced using the interaction potential developed by Gee et al.,⁴⁷ which shows pair radial distribution functions (RDF) close to those obtained by Edwards et al.⁴⁴ Hence, the RDFs obtained with the models proposed by Edwards et al.⁴⁴ and Gee et al.⁴⁷ were taken as reference to assess the accuracy of the AIMD results reported in the present work. Figure 8 shows RDFs for selected intermolecular interactions obtained with AIMD simulations of liquid acetonitrile performed with (i.e., BLYP-D3) and without (i.e., BLYP) van der Waals corrections. Although all of the AIMD simulations provided structural results in agreement with the reference models,^{44,47} simulations performed with the addition of the D3 dispersion interactions with the new refined

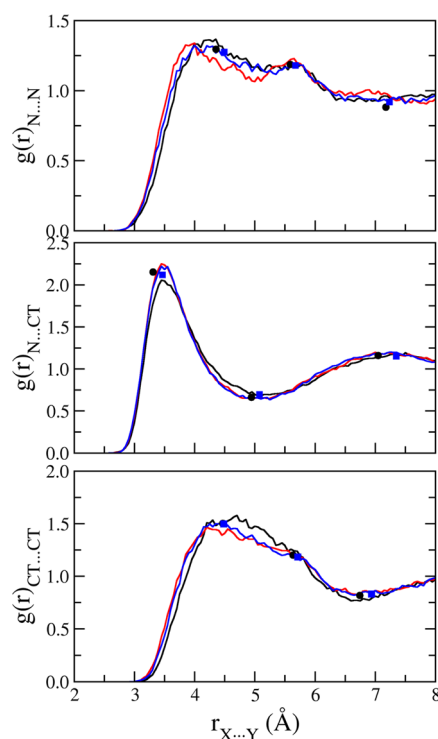


Figure 8. Radial distribution functions for selected intermolecular interactions in liquid acetonitrile (N = nitrogen atom; CT = carbon atom of the methyl group) as issued from AIMD simulations without (black) or with (red: default S_8 ; blue: optimized S_8) Grimme's D3 correction energy. Reference (experimental) RDF maxima and minima reported by Edwards et al.⁴⁴ and Gee et al.⁴⁷ are shown with black circles and blue squares, respectively.

S_8 parameter faithfully reproduced the positions of both maxima and minima.

Then, the effect on the pressure of the dispersion-corrected BLYP was assessed from calculation of the stress tensor on a series of configurations sampled every 0.1 ps during the AIMD simulations of liquid acetonitrile. Similar attempts were reported in previous studies of liquid water.^{17,18} Note that, as usual, pressure calculations of small molecular systems are characterized by very high fluctuations. Hence, according to standard practice, we considered the time evolution of the corresponding running average. In Figure 9, the pressure

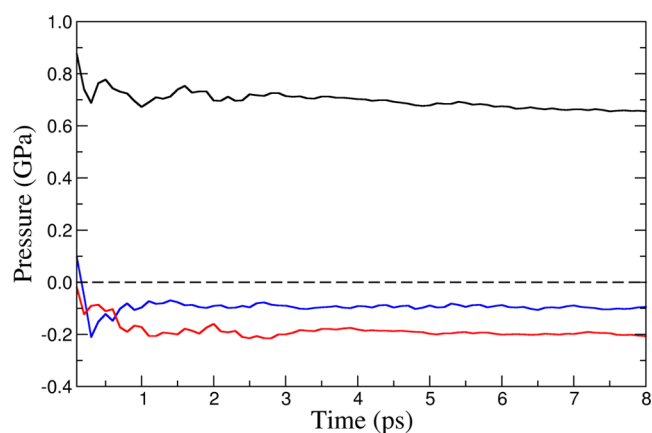


Figure 9. Pressure running average issued from AIMD simulations without (black) or with (red: default S_8 ; blue: optimized S_8) Grimme's D3 correction energy. Final average values of pressure are 0.657 ± 0.234 (uncorrected), -0.207 ± 0.205 (default S_8), and -0.095 ± 0.255 GPa (optimized S_8). The dashed line corresponds to ambient pressure (10^{-4} GPa).

running average is depicted as issued from all three AIMD simulations. It was observed that a rather high pressure (~ 0.6 GPa) was obtained in the simulation without dispersion corrections, suggesting that BLYP would underestimate the experimental density of acetonitrile. Inclusion of the D3 correction term was expected to decrease the computed pressure as a result of the enhanced attractive interactions. Indeed, the resulting pressure was significantly lower and somewhat negative for BLYP-D3 simulations, showing again that a better agreement with experiments (i.e., ambient pressure) was observed when employing the optimized D3 term accounting for the dispersion energy correction. This also suggests that BLYP-D3 would overestimate the density of liquid acetonitrile at normal conditions, a result somewhat in analogy to what was observed for liquid water by Ma et al.¹⁸ using Car–Parrinello MD simulations.

4. CONCLUSIONS

In the present work, we refined the parametrization of two very popular empirically dispersion-corrected DFT functionals, i.e., BLYP and B3LYP, aiming at improving the description of the interaction energy as occurring in molecular clusters of growing size and, ultimately, in condensed-phase systems. Our approach adopted the well tested and computationally efficient Grimme's D3 correction model and used diffusion quantum Monte Carlo calculations as a benchmark due to the statistically high accuracy of the latter (~ 0.1 kcal/mol). Note, however, that while keeping the same general idea, the present approach can be easily extended to other "versions" of the still growing family of DFT-D methods and/or to other purposely chosen reference calculations. For example, the more recent

D4 correction shares the same two-body dispersion term of D3, as expressed in eq 3. In particular, we performed benchmark calculations on a large set of molecular configurations of acetonitrile, ranging from dimers to hexadecamers. We believe this represents a key step of our computational protocol, since, on one hand, it allows to (over-)emphasize the possible flaws affecting both well-established or newly developed DFT-D models (e.g., under- or over-estimation of the London interactions), and, on the other hand, it helps to extrapolate the results to much larger molecular samples. The results showed that while the default D3 correction works surprisingly well, especially for the cost-effective BLYP functional, there was significant room for improvements on the computed interaction energy of medium-to-large-sized molecular systems, as compared to DMC data. By optimizing just one parameter of the D3 dispersion energy term, namely, the S_8 scaling factor of the $n = 8$ order term, we were able to decrease the observed MAE by a factor of 4, basically reaching the same accuracy of reference data (0.1 kcal/mol per molecule). Remarkably, the optimized D3 term was easily transferred to AIMD simulations of liquid acetonitrile, where small but non-negligible improvements in the structural (i.e., interatomic pair distribution functions) and thermodynamic (i.e., pressure) properties of the condensed-phase system were apparent, thus validating the extrapolation of parameters previously tailored toward molecular clusters of increasing size. Moreover, we would like to point out that the present protocol may benefit computationally from the use of newly developed DFT approximations optimized for small atomic orbital basis sets.⁴⁸

While we are aware that the optimization protocol outlined above is essentially system-dependent, meaning that the results are tailored specifically toward a given molecular system, we believe that this is an unavoidable necessity of an empirical correction aiming at high chemical accuracy. Yet, in our opinion, such a computational approach is simple and efficient enough to be applicable to a large number of chemical systems (including, for example, solute–solvent systems in which solvent interactions are optimized), whenever high accuracy is required. Indeed, the resulting dispersion corrections are readily transferable to widely used QM and AIMD software packages to perform cluster optimizations or MD simulations using either atomic orbital basis sets or plane waves.

■ ASSOCIATED CONTENT

Supporting Information

The Supporting Information is available free of charge at <https://pubs.acs.org/doi/10.1021/acs.jpca.1c07576>.

B3LYP energy deviations of acetonitrile 8mer configurations computed with default Grimme's D3 correction, without and with D3 correction including only the $n = 6$ order term (Figure S1); DFT-D3 energy deviations of acetonitrile 8mer configurations computed at B3LYP, BLYP, M062x, and B2PLYP level of theory (Figure S2); default DFT-D3, DFT-D3BJ, and DFT-D4 energy deviations of acetonitrile 8mer configurations computed at B3LYP and BLYP level of theory (Figure S3); B3LYP energy deviations of acetonitrile monomers computed with default Grimme's D3 correction (Figure S4); B3LYP-D3 interaction energy deviations with respect to DMC as computed with the 6-31+G(d,p), 6-31+D(2d,2p), aug-cc-pVTZ, and 6-31G* basis sets on

a set of acetonitrile 8mer cluster configurations (Figure S5); error, mean square error, mean absolute error, and MAE per molecule of default B3LYP-D3 and BLYP-D3 interaction energy deviations computed using the 6-31+G(d,p), 6-31+D(2d,2p), and aug-cc-pVTZ basis sets on all acetonitrile clusters (Table S1); mean absolute error of B3LYP-D3/6-31+G(d,p) interaction energy deviations with respect to DMC as computed by setting different S_8 scaling factors on a set of octamer cluster configurations (Table S2); mean absolute error of BLYP-D3/6-31+G(d,p) interaction energy deviations with respect to DMC as computed by setting different S_8 scaling factors on a set of octamer cluster configurations (Table S3) (PDF)

AUTHOR INFORMATION

Corresponding Author

Giuseppe Brancato – Scuola Normale Superiore and CSGI, I-56126 Pisa, Italy; Istituto Nazionale di Fisica Nucleare (INFN) sezione di Pisa, 56127 Pisa, Italy; orcid.org/0000-0001-8059-2517; Email: giuseppe.brancato@sns.it

Authors

Nuno Barbosa – Scuola Normale Superiore and CSGI, I-56126 Pisa, Italy

Marco Pagliai – Dipartimento di Chimica “Ugo Schiff”, Università degli Studi di Firenze, 50019 Sesto Fiorentino, Italy; orcid.org/0000-0003-0240-161X

Sourab Sinha – Scuola Normale Superiore and CSGI, I-56126 Pisa, Italy

Vincenzo Barone – Scuola Normale Superiore and CSGI, I-56126 Pisa, Italy; Istituto Nazionale di Fisica Nucleare (INFN) sezione di Pisa, 56127 Pisa, Italy; orcid.org/0000-0001-6420-4107

Dario Alfè – Department of Earth Sciences, Thomas Young Center, University College London, WC1E 6BS London, United Kingdom; London Centre for Nanotechnology, Thomas Young Centre, University College London, WC1H 0AH London, United Kingdom; Dipartimento di Fisica Ettore Pancini, Università di Napoli Federico II, 80126 Napoli, Italy; orcid.org/0000-0002-9741-8678

Complete contact information is available at: <https://pubs.acs.org/10.1021/acs.jpca.1c07576>

Notes

The authors declare no competing financial interest.

ACKNOWLEDGMENTS

This work was funded by MIUR through the PRIN program (contract no. 2012SK7ASN). Technical staff of the HPC Avogadro center is kindly acknowledged for managing the computing facilities at SNS.

ABBREVIATIONS

MD:molecular dynamics; AIMD:ab initio molecular dynamics; DMC:diffusion Monte Carlo

REFERENCES

(1) Berland, K.; Cooper, V. R.; Lee, K.; Schröder, E.; Thonhauser, T.; Hyldgaard, P.; Lundqvist, B. I. Van Der Waals Forces in Density Functional Theory: A Review of the VdW-DF Method. *Rep. Prog. Phys.* **2015**, *78*, No. 066501.

(2) Becke, A. D.; Johnson, E. R. A Density-Functional Model of the Dispersion Interaction. *J. Chem. Phys.* **2005**, *123*, No. 154101.

(3) Tkatchenko, A.; Scheffler, M. Accurate Molecular Van Der Waals Interactions from Ground-State Electron Density and Free-Atom Reference Data. *Phys. Rev. Lett.* **2009**, *102*, No. 073005.

(4) Grimme, S.; Antony, J.; Ehrlich, S.; Krieg, H. A Consistent and Accurate Ab Initio Parametrization of Density Functional Dispersion Correction (DFT-D) for the 94 Elements H-Pu. *J. Chem. Phys.* **2010**, *132*, No. 154104.

(5) Grimme, S.; Hansen, A.; Brandenburg, J. G.; Bannwarth, C. Dispersion-Corrected Mean-Field Electronic Structure Methods. *Chem. Rev.* **2016**, *116*, 5105–5154.

(6) Grimme, S. Accurate Description of van Der Waals Complexes by Density Functional Theory Including Empirical Corrections. *J. Comput. Chem.* **2004**, *25*, 1463–1473.

(7) Grimme, S. Semiempirical GGA-type density functional constructed with a long-range dispersion correction. *J. Comput. Chem.* **2006**, *27*, 1787–1799.

(8) Risthaus, T.; Grimme, S. Benchmarking of London Dispersion-Accounting Density Functional Theory Methods on Very Large Molecular Complexes. *J. Chem. Theory Comput.* **2013**, *9*, 1580–1591.

(9) Spicher, S.; Caldeweyher, E.; Hansen, A.; Grimme, S. Benchmarking London Dispersion Corrected Density Functional Theory for Noncovalent Ion- π Interactions. *Phys. Chem. Chem. Phys.* **2021**, *23*, 11635–11648.

(10) Becke, A. D. Density-functional Thermochemistry. III. The Role of Exact Exchange. *J. Chem. Phys.* **1993**, *98*, 5648–5652.

(11) Stephens, P. J.; Devlin, F. J.; Chabalowski, C. F.; Frisch, M. J. Ab Initio Calculation of Vibrational Absorption and Circular Dichroism Spectra Using Density Functional Force Fields. *J. Phys. Chem. A* **1994**, *98*, 11623–11627.

(12) Jurečka, P.; Šponer, J.; Černý, J.; Hobza, P. Benchmark Database of Accurate (MP2 and CCSD(T) Complete Basis Set Limit) Interaction Energies of Small Model Complexes, DNA Base Pairs, and Amino Acid Pairs. *Phys. Chem. Chem. Phys.* **2006**, *8*, 1985–1993.

(13) Grimme, S. Supramolecular Binding Thermodynamics by Dispersion-Corrected Density Functional Theory. *Chem. - Eur. J.* **2012**, *18*, 9955–9964.

(14) Otero-de-la-Roza, A.; Johnson, E. R. A Benchmark for Non-Covalent Interactions in Solids. *J. Chem. Phys.* **2012**, *137*, No. 054103.

(15) Ambrosetti, A.; Alfè, D.; DiStasio, R. A.; Tkatchenko, A. Hard Numbers for Large Molecules: Toward Exact Energetics for Supramolecular Systems. *J. Phys. Chem. Lett.* **2014**, *5*, 849–855.

(16) Brandenburg, J. G.; Zen, A.; Fitzner, M.; Ramberger, B.; Kresse, G.; Tsatsoulis, T.; Grüneis, A.; Michaelides, A.; Alfè, D. Physorption of Water on Graphene: Subchemical Accuracy from Many-Body Electronic Structure Methods. *J. Phys. Chem. Lett.* **2019**, *10*, 358–368.

(17) Schmidt, J.; VandeVondele, J.; Kuo, I.-F. W.; Sebastiani, D.; Siepmann, J. I.; Hutter, J.; Mundy, C. J. Isobaric–Isothermal Molecular Dynamics Simulations Utilizing Density Functional Theory: An Assessment of the Structure and Density of Water at Near-Ambient Conditions. *J. Phys. Chem. B* **2009**, *113*, 11959–11964.

(18) Ma, Z.; Zhang, Y.; Tuckerman, M. E. Ab Initio Molecular Dynamics Study of Water at Constant Pressure Using Converged Basis Sets and Empirical Dispersion Corrections. *J. Chem. Phys.* **2012**, *137*, No. 044506.

(19) Caldeweyher, E.; Bannwarth, C.; Grimme, S. Extension of the D3 Dispersion Coefficient Model. *J. Chem. Phys.* **2017**, *147*, No. 034112.

(20) Caldeweyher, E.; Ehlert, S.; Hansen, A.; Neugebauer, H.; Spicher, S.; Bannwarth, C.; Grimme, S. A Generally Applicable Atomic-Charge Dependent London Dispersion Correction. *J. Chem. Phys.* **2019**, *150*, No. 154122.

(21) Nikitin, A. M.; Lyubartsev, A. P. New Six-Site Acetonitrile Model for Simulations of Liquid Acetonitrile and Its Aqueous Mixtures. *J. Comput. Chem.* **2007**, *28*, 2020–2026.

- (22) Hess, B.; Bekker, H.; Berendsen, H. J. C.; Fraaije, J. G. E. M. LINC: A Linear Constraint Solver for Molecular Simulations. *J. Comput. Chem.* **1997**, *18*, 1463–1472.
- (23) Berendsen, H. J. C.; van der Spoel, D.; van Drunen, R. GROMACS: A Message-Passing Parallel Molecular Dynamics Implementation. *Comput. Phys. Commun.* **1995**, *91*, 43–56.
- (24) Needs, R. J.; Towler, M. D.; Drummond, N. D.; López Ríos, P. Continuum Variational and Diffusion Quantum Monte Carlo Calculations. *J. Phys.: Condens. Matter* **2010**, *22*, No. 023201.
- (25) Mitáš, L.; Shirley, E. L.; Ceperley, D. M. Nonlocal Pseudopotentials and Diffusion Monte Carlo. *J. Chem. Phys.* **1991**, *95*, 3467–3475.
- (26) Casula, M. Beyond the Locality Approximation in the Standard Diffusion Monte Carlo Method. *Phys. Rev. B* **2006**, *74*, No. 161102.
- (27) Trail, J. R.; Needs, R. J. Smooth Relativistic Hartree–Fock Pseudopotentials for H to Ba and Lu to Hg. *J. Chem. Phys.* **2005**, *122*, No. 174109.
- (28) Baroni, S.; de Gironcoli, S.; Dal Corso, A.; Giannozzi, P. Phonons and Related Crystal Properties from Density-Functional Perturbation Theory. *Rev. Mod. Phys.* **2001**, *73*, 515–562.
- (29) Alfè, D.; Gillan, M. J. Efficient Localized Basis Set for Quantum Monte Carlo Calculations on Condensed Matter. *Phys. Rev. B* **2004**, *70*, No. 161101.
- (30) Frisch, M. J.; Trucks, G. W.; Schlegel, H. B.; Scuseria, G. E.; Robb, M. A.; Cheeseman, J. R.; Scalmani, G.; Barone, V.; Mennucci, B.; Petersson, G. A.; et al. *Gaussian 09*; Gaussian Inc.: Wallingford, CT, 2009.
- (31) Becke, A. D. Density-Functional Exchange-Energy Approximation with Correct Asymptotic Behavior. *Phys. Rev. A* **1988**, *38*, 3098–3100.
- (32) Lee, C.; Yang, W.; Parr, R. G. Development of the Colle-Salvetti Correlation-Energy Formula into a Functional of the Electron Density. *Phys. Rev. B* **1988**, *37*, 785–789.
- (33) Miehlich, B.; Savin, A.; Stoll, H.; Preuss, H. Results Obtained with the Correlation Energy Density Functionals of Becke and Lee, Yang and Parr. *Chem. Phys. Lett.* **1989**, *157*, 200–206.
- (34) Becke, A. D. Density-Functional Thermochemistry. III. The Role of Exact Exchange. *J. Chem. Phys.* **1993**, *98*, No. 5648.
- (35) Dunning, T. H. Gaussian Basis Sets for Use in Correlated Molecular Calculations. I. The Atoms Boron through Neon and Hydrogen. *J. Chem. Phys.* **1989**, *90*, 1007–1023.
- (36) Grimme, S.; Ehrlich, S.; Goerigk, L. Effect of the Damping Function in Dispersion Corrected Density Functional Theory. *J. Comput. Chem.* **2011**, *32*, 1456–1465.
- (37) VandeVondele, J.; Krack, M.; Mohamed, F.; Parrinello, M.; Chassaing, T.; Hutter, J. Quickstep: Fast and Accurate Density Functional Calculations Using a Mixed Gaussian and Plane Waves Approach. *Comput. Phys. Commun.* **2005**, *167*, 103–128.
- (38) Hutter, J.; Iannuzzi, M.; Schiffmann, F.; VandeVondele, J. Cp2k: Atomistic Simulations of Condensed Matter Systems: Cp 2 k Simulation Software. *Wiley Interdiscip. Rev.: Comput. Mol. Sci.* **2014**, *4*, 15–25.
- (39) Goedecker, S.; Teter, M.; Hutter, J. Separable Dual-Space Gaussian Pseudopotentials. *Phys. Rev. B* **1996**, *54*, 1703–1710.
- (40) Bertagnolli, H.; Chieux, P.; Zeidler, M. D. A Neutron-Diffraction Study of Liquid Acetonitrile: I. CD 3 C 14 N. *Mol. Phys.* **1976**, *32*, 759–773.
- (41) Bertagnolli, H.; Zeidler, M. D. Molecular Pair-Correlation Function of Liquid Acetonitrile from X-Ray and Neutron-Diffraction Studies. *Mol. Phys.* **1978**, *35*, 177–192.
- (42) Böhm, H. J.; McDonald, I. R.; Madden, P. A. An Effective Pair Potential for Liquid Acetonitrile. *Mol. Phys.* **1983**, *49*, 347–360.
- (43) Böhm, H. J.; Meissner, C.; Ahlrichs, R. Molecular Dynamics Simulation of Liquid CH 3 F, CHF 3, CH 3 Cl, CH 3 CN, CO 2 and CS 2 with New Pair Potentials. *Mol. Phys.* **1984**, *53*, 651–672.
- (44) Edwards, D. M. F.; Madden, P. A.; McDonald, I. R. A Computer Simulation Study of the Dielectric Properties of a Model of Methyl Cyanide: I. The Rigid Dipole Case. *Mol. Phys.* **1984**, *51*, 1141–1161.
- (45) Jorgensen, W. L.; Briggs, J. M. Monte Carlo Simulations of Liquid Acetonitrile with a Three-Site Model. *Mol. Phys.* **1988**, *63*, 547–558.
- (46) Guàrdia, E.; Pinzón, R.; Casulleras, J.; Orozco, M.; Luque, F. J. Comparison of Different Three-Site Interaction Potentials for Liquid Acetonitrile. *Mol. Simul.* **2001**, *26*, 287–306.
- (47) Gee, P. J.; van Gunsteren, W. F. Acetonitrile Revisited: A Molecular Dynamics Study of the Liquid Phase. *Mol. Phys.* **2006**, *104*, 477–483.
- (48) Grimme, S.; Brandenburg, J. G.; Bannwarth, C.; Hansen, A. Consistent Structures and Interactions by Density Functional Theory with Small Atomic Orbital Basis Sets. *J. Chem. Phys.* **2015**, *143*, No. 054107.